Propagation and amplification of short radio-frequency pulses in a plasma channel created in gaseous media by the intense laser radiation

A V Bogatskaya[1,2,3], A M Popov[1,2,3], I V Smetanin[3] and E A Volkova[1]
[1] D.V. Skobeltsyn Institute of Nuclear Physics, Moscow State University, Moscow, Russia
[2] Department of Physics, Moscow State University, Moscow, Russia
[3] P.N. Lebedev Physical Institute, RAS, Moscow, Russia

E-mail: annabogatskaya@gmail.com

Abstract. The evolution of the electron energy distribution function (EEDF) in non-equilibrium plasma channel created in xenon by powerful KrF - femtosecond laser pulse is studied. It is demonstrated that such a plasma channel can be used as a waveguide for both transportation and amplification of the microwave radiation. The specific features of such a plasma waveguide are studied on the basis of the self-consistent solution of the kinetic Boltzmann equation for the EEDF in different spatial points of the gas media and the wave equation in slow-varying amplitude approximation for the microwave radiation guided and amplified in the channel.

1. Introduction

Impressive progress in high-power ultrashort laser techniques makes it possible to create long plasma channels in different gaseous media. The formation of a plasma channel by a high-intensity femtosecond laser pulses arises mainly from the process of multiphoton ionization of gas atoms and molecules, therefore the electron energy spectrum of such an plasma channel consists of a set of peaks, the positions of which are determined by absorption of certain quanta of energy. The specific electrodynamic features of such plasma structures cause particular interest in them for a number of applications, including generation of XUV attosecond pulses [1,2], triggering of high-voltage discharges [3-6], remote sensing of the atmosphere [7] and long distance transportation of microwave radiation [8,9]. In [10] it was proposed that such a plasma channel with strong nonequilibrium of the electron subsystem could be used to amplify electromagnetic radiation in a microwave frequency band. The possibility of using electron energy distribution functions (EEDF) containing an inverse population to amplify electromagnetic radiation was first discussed in [11,12]. The detailed analysis of EEDF relaxation in a plasma channel created by a femtosecond KrF laser pulse and calculation of the gain factor in dependence on initial plasma parameters and on the intensity and frequency of the RF radiation in a number of atomic and molecular gases is given in [13]. In particular, it was found that among both atomic and molecular gases that can be used for amplification of the RF radiation xenon plasma has some advantages. The time interval of the positive gain factor existence is the largest for xenon plasma and can reach hundreds of nanoseconds.

In this paper we discuss the fact that a strong nonequilibrium of photoelectron spectrum can also lead to unusual refractive properties of the plasma channel forming in the process of multiphoton ionization of gas media by femtosecond laser pulse. In particular, the real part of plasma permittivity can become larger than unity, i.e. plasma turns out to be optically more dense medium in comparison with the surrounding unionized gas. The aforesaid provides the possibility to use such a channel as a waveguide which enable to maintain both transportation and amplification of the microwave radiation. The process of guiding and amplification of the microwave radiation in the plasma channel formed by powerful KrF laser femtosecond pulse in xenon is studied numerically on the basis of the self-consistent solution of the Boltzmann equation for the electron energy distribution function (EEDF) evolution in the nonequlibrium plasma and the wave equation for the transported through the channel RF pulse. The conditions of effective propagation and amplification of the RF pulse in a plasma waveguide are discussed.

2. Photoionization by the ultrashort UV laser pulse. Multiphoton ionization

At first we consider the formation of a plasma channel in the process of photoionization of gas atoms by the femtosecond UV laser pulse. At figure 1 numerical calculations of the Schrodinger equation for probabilities of ionization (per pulse) of xenon and argon atoms are shown. For intensities of laser pulse 10^{12}-10^{14} W/cm^2 in accordance with the perturbation theory the ionization probability of xenon atoms is described by a cubic dependence on the radiation intensity. As regards to argon atoms, we have four-photon ionization therefore the dependence of ionization probability is four-power. In argon we can also observe saturation of the ionization probability, which is caused by the population trapping of the Rydberg states of atoms [14]. Figure 2 demonstrates the typical photoelectron spectra formed by the multihoton ionization of xenon and argon atoms. For intensities less than 10^{13} W/cm^2 the Stark shift of the continuum can be neglected, therefore the position of the first peak in the xenon energy spectrum corresponding to the absorption of three photons is determined by the energy $\varepsilon_0 = 3\hbar\omega - I_i$, I_i is the ionization potential for xenon atoms. In the case of argon atoms we have $\varepsilon_0 = 4\hbar\omega - I_i$. Above-threshold ionization peaks are negligible for such a range of radiation intensities. Therefore in fact we obtain one pronounced peak which evolves due to elastic and inelastic processes in plasma.

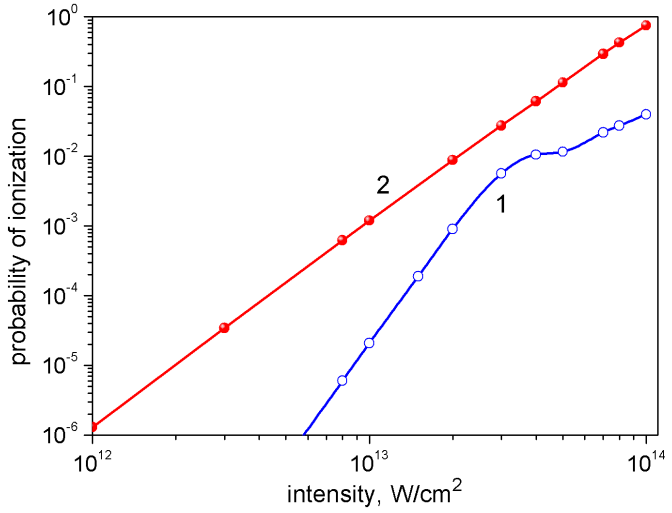

Figure 1. Ionization probabilities v_i of argon (*1*) and xenon (*2*) atoms per pulse as functions of intensity I of laser radiation with λ = 248 nm.

It is worth to note that for such pulse durations (about 100 fs) the characteristic time between electron-atomic collisions which can be estimated as $T_c \approx 1/N\sigma v \sim 3\times10^{-13}$ s (here $N \cong 3\times10^{19}$ cm^{-3}

is the density of atoms (molecules) at the atmospheric pressure, $\sigma \cong 10^{-15}$ cm^2 is the collision cross section and $v \sim 10^8$ cm/s is the velocity of electrons resulting from photoionization) is more than the duration of the laser pulse. This signifies that the photoelectron energy spectrum created by the laser pulse no longer than 300 fs is determined only by the photoionization dynamics of gas atoms (molecules) and the evolution of the energy spectrum which is described by the Boltzmann equation takes place in the postpulse regime.

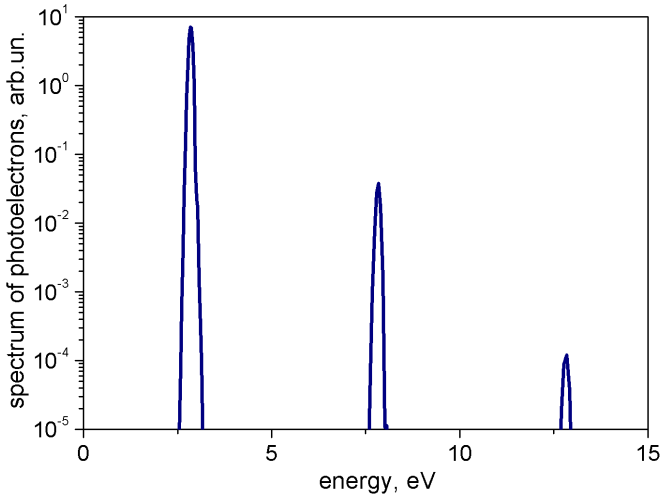

Figure 2. Photoelectron spectra in xenon for a radiation intensity $I = 10^{13}$ W/cm^2.

3. Boltzmann equation for the evolution of the EEDF

Evolution of the plasma channel with nonequilibrium EEDF can be studied using the kinetic Boltzmann equation:

$$\frac{\partial n(\varepsilon,t)}{\partial t}\sqrt{\varepsilon} = \frac{\partial}{\partial \varepsilon}\left(\frac{e^2 E_0^2 \nu_{tr}(\varepsilon)}{3m(\omega^2+\nu_{tr}^2)}\varepsilon^{3/2}\frac{\partial n}{\partial \varepsilon}\right) + \frac{2m}{M}\frac{\partial}{\partial \varepsilon}\left(\nu_{tr}(\varepsilon)\varepsilon^{3/2}\left(n(\varepsilon,t)+T_g\frac{\partial n(\varepsilon,t)}{\partial \varepsilon}\right)\right) + Q_{ee}(n) + Q^*(n). \quad (1)$$

As for physical meaning of equation (1) it describes the diffusion process in the energy space. The first term stands for the influence of the transported RF field with frequency ω and the amplitude of electric field strength E_0, the second represents elastic losses of energy, the third one describes the effect of the gas temperature. Here T_g is the gas temperature (we assume $T_g \approx 0.03$ eV), m is the mass of electron, M is the mass of gas atom, $\nu_{tr}(v) = N\sigma_{tr}v$, σ_{tr} are the transport frequency and scattering cross section of electron-atomic collisions correspondingly. Last two terms of equation (1) are the integrals of electron-electron collisions $Q_{ee}(n)$ and inelastic collisions $Q^*(n)$. It is important to mention that in rare gases the energy lowest excitation thresholds for electronic states are equal to 8.31 eV for xenon atoms and 11.5 eV for argon atoms. This is significantly higher than the energy peak corresponding to the photoelectrons produced by the femtosecond laser pulse. Under the conditions involved, evolution of the energy spectrum in rare gases is determined by elastic and electron-electron collisions and by the influence of transported RF field. For the numerical analysis of Boltzmann equation we approximate the initial photoelectron peak by the Gaussian shape:

$$n(\varepsilon, t=0) = \frac{1}{\Delta\varepsilon\sqrt{\pi\varepsilon}}\exp\left(-\frac{(\varepsilon-\varepsilon_0)^2}{(\Delta\varepsilon)^2}\right) \quad (2)$$

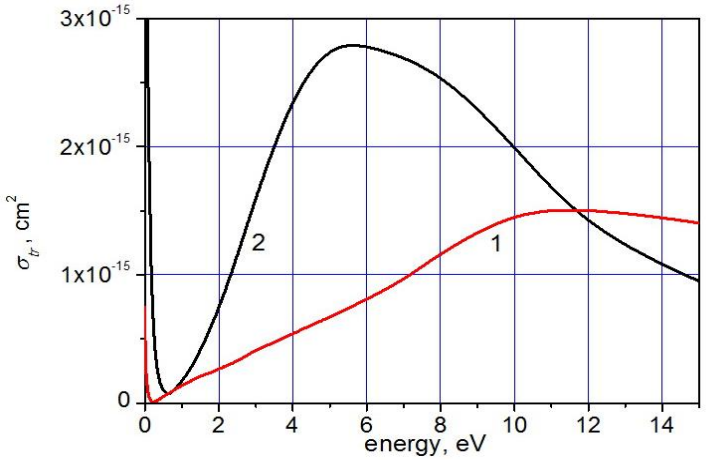

Figure 3. Transport scattering cross sections for argon (1) and xenon (2) atoms.

Figure 3 shows dependences of transport cross sections for xenon and argon atoms. Such rare gases are characterized by a Ramsauer minimum and as a consequence by the ranges of rapidly growing transport cross sections. It has to be emphasized that initial peak is located namely in the range of rapidly growing values of cross section. The numerical solutions of Boltzmann equation in xenon and argon obtained under the assumption that electron-electron collisions and RF field do not contribute to the evolution of the EEDF are presented at figure 4. It is clearly seen that in this case the initial peak gradually shifts towards lower energies keeping approximately the Gaussian shape and also one can notice the retardation of the velocity of peak displacement. Here the diffusion spreading is negligible, furthermore, the lowering of elastic collision frequency ν_{tr} with the deceleration of electrons leads to the opposite effect – the narrowing of the peak.

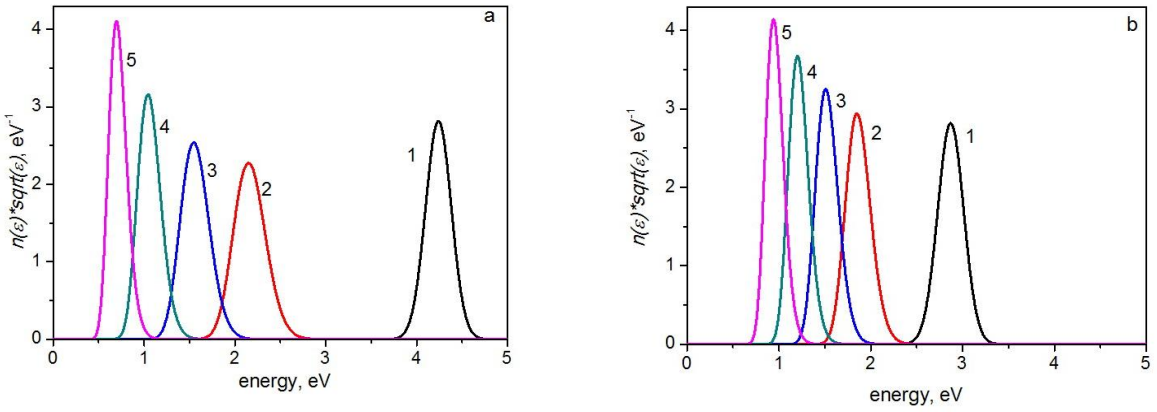

Figure 4. EEDF for argon (a) and xenon (b) at the instants of time (*1*) 0, (*2*) 25, (*3*) 50, (*4*) 100, and (*5*) 200 ns after plasma channel production by λ = 248 nm laser radiation.

4. Optical properties of the plasma channel

The knowledge of the EEDF makes it possible to obtain some optical properties of a plasma channel. The complex conductivity of plasma can be written in the following form [4]:

$$\sigma(\omega)=\sigma'+i\sigma''=\frac{2}{3}\frac{e^2N_e}{m}\int_0^\infty\frac{\varepsilon^{3/2}(\nu_{tr}(\varepsilon)+i\omega)}{\omega^2+\nu_{tr}^2(\varepsilon)}\left(-\frac{\partial n(\varepsilon,t)}{\partial\varepsilon}\right)d\varepsilon. \qquad (3)$$

where N_e is the concentration of electrons in plasma. The real part of plasma conductivity stands for the energy dissipation in plasma; therefore we have the expression for the absorption coefficient:

$$\mu_\omega = \frac{4\pi\sigma'}{c} = \frac{8\pi}{3}\frac{e^2 N_e}{mc}\int_0^\infty \frac{\varepsilon^{3/2}\nu_{tr}(\varepsilon)}{\omega^2+\nu_{tr}^2(\varepsilon)}\left(-\frac{\partial n(\varepsilon,t)}{\partial\varepsilon}\right)d\varepsilon. \quad (4)$$

The EEDF usually decreases with the increase of energy, i.e. $\partial n/\partial\varepsilon < 0$ and consequently the value of integral (4) is positive: $\sigma' > 0$ and $\mu_\omega > 0$. However, the electron energy distribution which arises from the photoionization process contains energy ranges with the positive value of derivative $\partial n/\partial\varepsilon$, making a negative contribution to the integral (4). In [13] authors drew attention to the fact that in low-frequency range the value of absorption coefficient may become even negative in rare gases with a pronounced Ramsauer effect. In that case the medium is capable to amplify RF radiation and the amplification condition can be represented in the following form:

$$\frac{d}{d\varepsilon}\left(\frac{\varepsilon^{3/2}\nu_{tr}}{\omega^2+\nu_{tr}^2}\right) < 0\ . \quad (5)$$

To obtain amplification in plasma the above condition should be fulfilled in the range of photoionization peak existence. When $\omega << \nu_{tr}$ one can obtain from (5):

$$\frac{d}{d\varepsilon}\varepsilon/\sigma_{tr} < 0, \quad (6)$$

which means that the transport cross section should increase with the energy faster than line dependence. Figure 5 shows the dependences $\sigma_{tr}(\varepsilon)/\varepsilon$ for xenon and argon atoms. One can figure out than xenon is more preferable as an amplifying media in comparison with argon. Actually, in xenon the amplification condition (6) is fulfilled in energy range of 1-4 eV, whereas for argon atoms the amplification effect may appear only for slow electrons in a narrow energy range $\varepsilon = 0.6-0.8$, which is hard to realize experimentally.

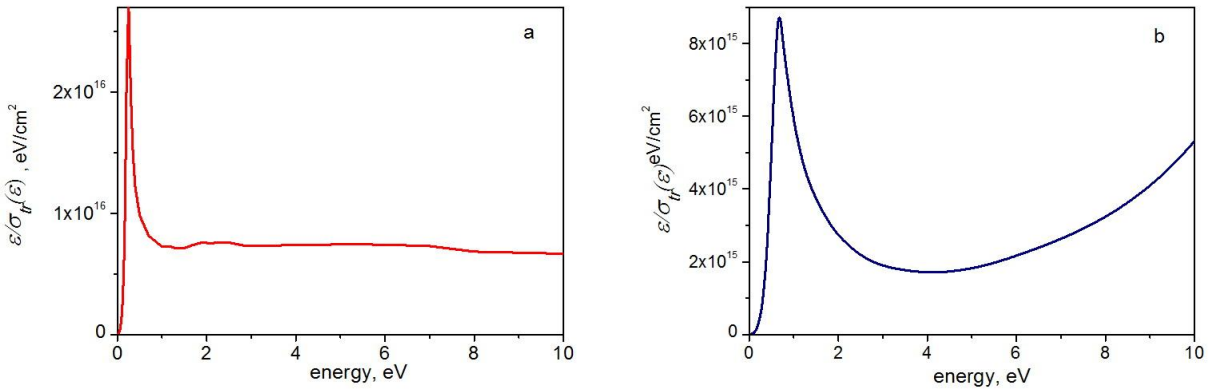

Figure 5. $\sigma_{tr}(\varepsilon)/\varepsilon$ as a function of electron energy for argon (a) and xenon (b) atoms.

In this work we would also like to pay attention to the fact that the inverse population of the EEDF also influences on the sign of the imaginary part of plasma conductivity (see equation (3)), which determines refraction features of a plasma channel. The common knowledge is that permittivity of weakly ionized plasma is less than unity, but in our case plasma channel with the nonequilibrium distribution function can be optically denser medium in comparison with unionized gas. We need the following inequality to be satisfied:

$$\frac{d}{d\varepsilon}\left(\frac{\varepsilon^{3/2}}{\omega^2+\nu_{tr}^2}\right) < 0, \quad (7)$$

which can be simplified in the low-frequency range: $\frac{d}{d\varepsilon}\varepsilon^{1/4}/\sigma_{tr} < 0$. The obtained result leads to the possibility to use such a plasma channel as a dielectric waveguide maintaining both effective transportation and amplification of RF radiation. The propagation process in a plasma channel is schematically shown at figure 6 and is based on the effect of total internal reflection at the interface with a unionized gas as an optically less dense medium [10].

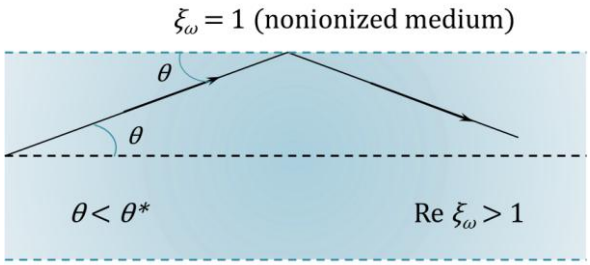

Figure 6. The sliding-mode waveguide scheme, θ is the angle of total internal reflection.

5. Analytics for optical properties of a plasma channel

In this section we discuss some analytics describing optical properties of a plasma channel. Dependences of transport cross sections in considered energy ranges can be approximated by power functions (see figure 7). We have the squared dependence of energy for xenon and a liner dependence for argon atoms, i.e. $\sigma_{tr}(\varepsilon) = \sigma_0(\varepsilon/\varepsilon_0)^\alpha$, where $\sigma_0 = 1.24\times10^{-15}$ см$^{-2}$, $\varepsilon_0 = 2.6$ eV, α = 2 for Xe and $\sigma_0 = 2.3\times10^{-16}$ см$^{-2}$, $\varepsilon_0 = 1.7$ eV, α = 1 for Ar.

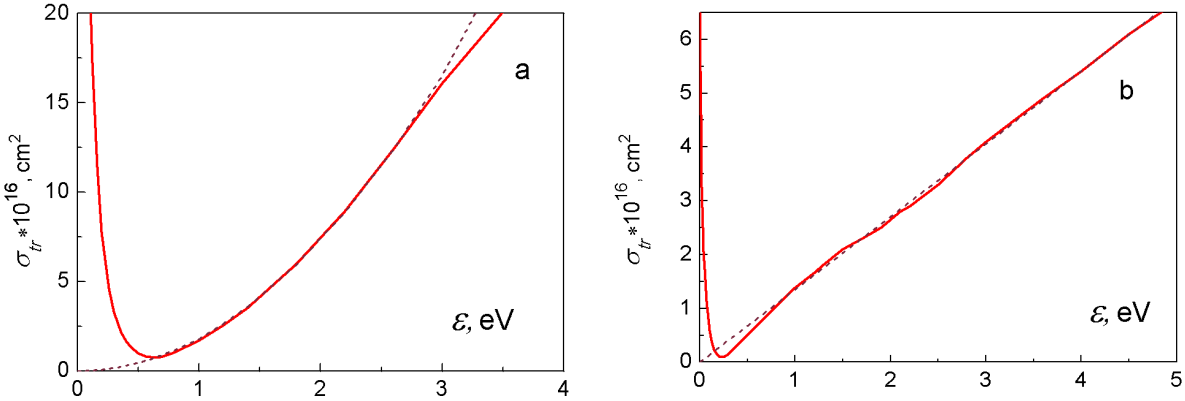

Figure 7. Transport scattering cross section (solid line) and its approximation (dashed line) in xenon (a) and argon (b).

In view of previous calculations of the EEDF evolution for qualitative analysis it is possible to assume the EEDF as a gradually shifted δ - peak, the temporal evolution of which is determined by the averaged over the spectrum energy of photoelectrons $\langle\varepsilon\rangle$:

$$\frac{d\langle\varepsilon\rangle}{dt} = -\frac{2m}{M}\nu_{tr}(\langle\varepsilon\rangle)\langle\varepsilon\rangle. \tag{8}$$

We can find the averaged energy $\langle\varepsilon\rangle$ also analytically:

$$\langle\varepsilon(t)\rangle = \frac{\langle\varepsilon(t=0)\rangle}{\left(1+\frac{2m}{M}(\alpha+1/2)\nu(t=0)t\right)^{1/(\alpha+1/2)}}. \tag{9}$$

As a result, using the δ - function properties we can easily obtain such expressions for the real and imaginary parts of plasma permittivity $\xi_\omega = \mathrm{Re}\,\xi_\omega + i\,\mathrm{Im}\,\xi_\omega$:

$$\mathrm{Re}\,\xi_\omega = 1 - \frac{\omega_p^2}{\omega^2 + \nu^2(t)} \frac{\omega^2 - \frac{2}{3}(2\alpha - 1/2)\nu^2(t)}{\omega^2 + \nu^2(t)}, \tag{10}$$

$$\mathrm{Im}\,\xi_\omega = \frac{2}{3} \frac{\omega_p^2 \nu(t)}{(\omega^2 + \nu^2(t))\omega} \frac{(\alpha + 2)\omega^2 + (1-\alpha)\nu^2(t)}{\omega^2 + \nu^2(t)}. \tag{11}$$

Here ω_p^2 is the plasma frequency squared and $\nu(t) = \nu_{tr}(\langle\varepsilon(t)\rangle)$. In the low-frequency range ($\omega << \nu_{tr}$) one can simplify the expressions:

$$\mathrm{Re}\,\xi_\omega \approx 1 + \frac{2}{3}\frac{\omega_p^2}{\nu^2(t)}(2\alpha - 1/2) > 1 \quad \text{if } \alpha > 1/4, \tag{12}$$

$$\mathrm{Im}\,\xi_\omega \approx \frac{2}{3}\frac{\omega_p^2}{\nu(t)\omega}(1-\alpha) < 0 \quad \text{if } \alpha > 1. \tag{13}$$

It can be seen that the condition of effective propagation regime (12) is less strict that the amplification condition (13).

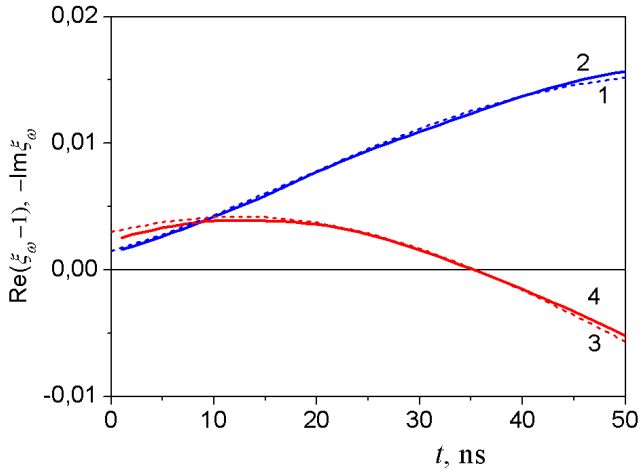

Figure 8. Time dependences of $\mathrm{Re}(\xi_\omega - 1)$ (1,2) and $-\mathrm{Im}\,\xi_\omega$ (3,4) in xenon obtained by analytical expressions (10), (11) (dashed line) and by numerical calculations (solid line), $n_e = 3\times10^{12}\mathrm{cm}^{-3}$.

We provide the comparison between the analytics and numerical calculation for real and imaginary parts of permittivity for RF frequency $\omega = 5\times10^{11}$ s^{-1} at figure 8. One can see rather good agreement. As the imaginary part of permittivity determines the absorption (amplification) coefficient, one can observe the amplification zone and much more prolonged guiding zone in the plasma channel.

6. Electron – electron collisions and RF field influence on the evolution of the EEDF

The influence of the electron – electron collisions was not taken into account in the previous discussion. We can estimate, that the characteristic value of energy exchange in ee-collisions is about $\Delta\varepsilon_{ee} \sim \varepsilon$. The characteristic energy losses in electron – atomic collisions are about four orders of value less: $\Delta\varepsilon_{ea} \sim \frac{2m}{M}\varepsilon$. Thus, during the ee – collisions the effective energy exchange takes place even for rather low degrees of ionization.

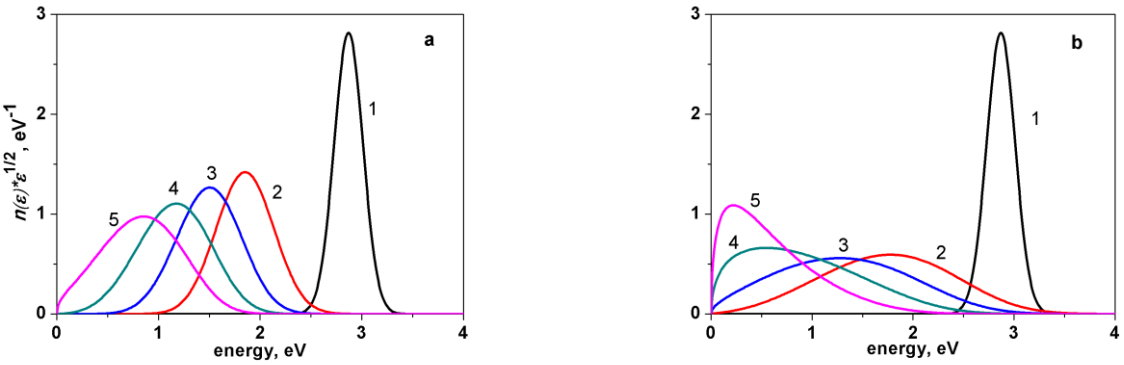

Figure 8. EEDF in xenon at the instants of time t=0 (1), t=25 (2), t=50 (3), t=100 (4), t=200 (5) ns after creation of the plasma channel by λ=248 nm radiation for electron densities 10^{12} (a) and 10^{13} cm^{-3} (b).

This process results in the fast maxwellization of the energy spectrum. The calculations confirm our predictions (see figure 8). As a result, that at the rather small instants of time the gain factor increases proportionally to the electron concentration, but the duration of the amplification in plasma decreases with the increase of N_e because of the speed up in relaxation of the EEDF.

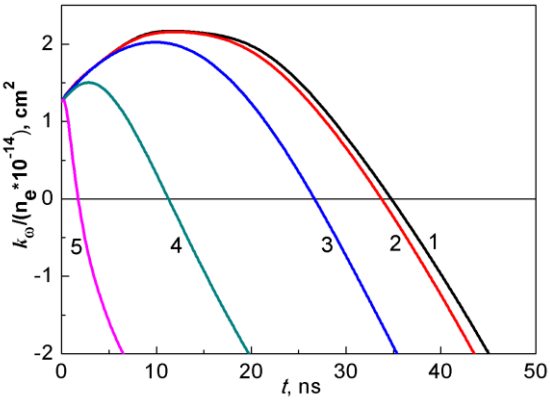

Figure 9. The gain factor per one electron in xenon plasma for different electronic densities (cm^{-3}): 1 - 10^{10}, 2 - 10^{11}, 3 - 10^{12}, 4 - 10^{13}, 5 - 10^{14}. Negative values correspond to the absorption on the RF radiation in plasma.

All the data discussed above were in the case when transported RF field doesn't influence on the evolution of the EEDF. Simple estimations reveal that one can neglect this influence if the relation $\frac{e^2E_0^2}{3m\nu_{tr}^2} < \max\left\{\frac{2m}{M}T_g, \langle\varepsilon\rangle\frac{\nu_{ee}}{\nu_{tr}}\right\}$ is fulfilled. For $\langle\varepsilon\rangle \approx 2$ eV and $n_e = 3\times10^{12}$ cm^{-3} above inequality is valid for intensities less than 100 W/cm^2. The figure 10 show that the more intense RF field results in faster spreading of the initial peak due to the diffusion of electrons in energy space.

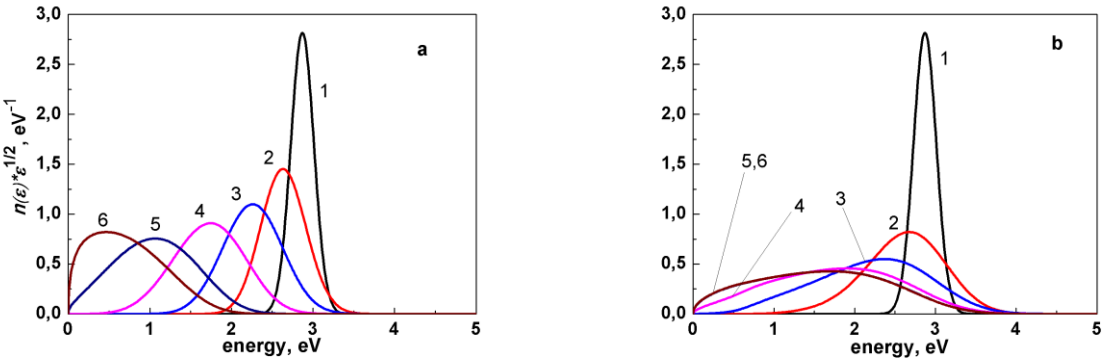

Figure 10. EEDF in xenon plasma at the instants of time t=0 (1), t=25 (2), t=50 (3), t=100 (4), t=200 (5) ns after the channel formation for RF field intensities (a) 0 and (b) 100 W/cm^2. Electronic density $N_e = 3\times10^{12}$ cm^{-3}.

The temporal evolution of averaged electron energy and the gain factor $k_\omega = -\mu_\omega$ for different values of the RF intensity is presented at figure 11. One can find out that the RF field presence leads to the additional cooling of the electron component of plasma which means the amplification if the RF signal. But with the increase of the RF field intensity the shortening of EEDF relaxation time takes place. This reduces the duration of the amplification (see figure 11a).

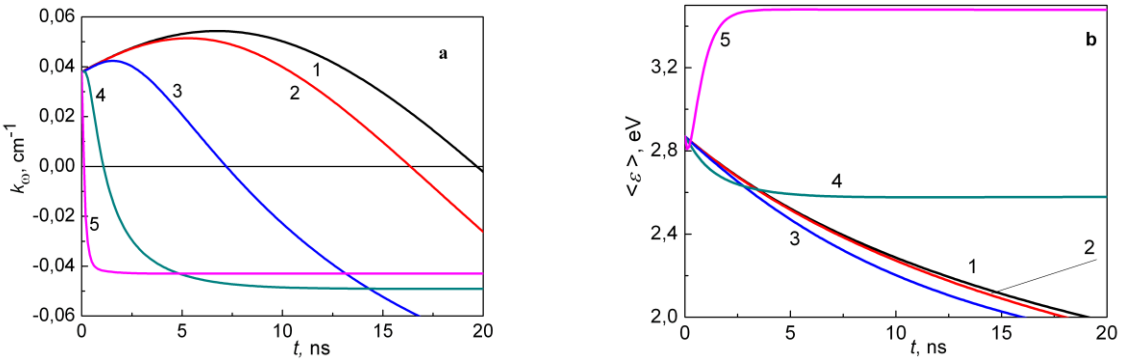

Figure 11. Time dependence of the gain factor of the electromagnetic radiation (a) and the average electron energy $\langle\varepsilon\rangle$ (b) for different intensities of the RF radiation: I=0 W/cm^2 (1), 10 W/cm^2 (2), 100 W/cm^2 (3), 10^3 W/cm^2 (4), 10^4 W/cm^2 (5). The data obtained for electronic density $n_e = 3\times10^{12}$ cm^{-3} and $\omega = 5\times10^{11}$ s^{-1}.

7. Propagation of the radio-frequency pulses in the plasma channel

In this chapter we will discuss the possibility to use the plasma channel as a waveguide for transportation and amplification of the RD radiation pulse. Our analysis is based on the self-consistent solution of the wave equation for the RF pulse and the Boltzmann equation for the EEDF in the plasma channel in different spatial points.

As it is known, propagation of the electromagnetic radiation in a medium is described by the wave equation:

$$\nabla^2\vec{E}(\vec{r},t) - \frac{1}{c^2}\frac{\partial^2\vec{E}}{\partial t^2} = \frac{4\pi}{c^2}\frac{\partial\vec{j}(\vec{r},t)}{\partial t}. \qquad (14)$$

Here $\vec{E}$ is the electric field strength and $\vec{j}$ is the density of the electric current in a plasma. Further we will suppose the field is linearly polarized. To analyze the process of RF pulse propagation qualitatively we use the slow-varying amplitude and phase (SVAP) approximation for the solution of equation (14). According to this approximation for the pulse propagation along *z*-direction electric field *E* should be represented as

$$E(\vec{r},t) = E_0(\rho,z,t)\cdot\exp\left(i\left(kz-\omega t\right)\right). \qquad (15)$$

Here E_0 is the envelope of the RF pulse, $k=\omega/c$ is the wave number and ρ is perpendicular spatial coordinate.

Neglecting the temporal dispersion it is possible to write down the following expression for the density of the electric current in plasma $j(\vec{r},t)=\sigma E(\vec{r},t)$ is the plasma conductivity. We also assume that the σ is slow varying function in space and time. Then using the SVAP approximation one can obtain the following equation for the electric pulse envelope

$$ik\left(\frac{\partial E_0}{\partial z}+\frac{1}{c}\left(1+i\frac{2\pi\sigma}{\omega}\right)\frac{\partial E_0}{\partial t}\right)=-\frac{1}{2}\nabla_\perp^2 E_0-\Delta n_\omega(t-z/c)k^2E_0+\frac{i}{2}k_\omega(t-z/c)\,kE_0. \qquad (16)$$

Here $\Delta n_\omega=\mathrm{Re}(n_\omega-1)=-\dfrac{2\pi\sigma''}{\omega}>0$. The first term in the right part of the equation stands for the diffraction divergence of the pulse, the second one describes the refractive properties of plasma. In our case we have refractive index greater than unity, so plasma channel reveals the focusing features. The third term represents amplification or absorption of the RF radiation.

The propagation process is schematically shown at figure 12. The femtosecond laser pulse creates a plasma channel which is characterized by the amplifying zone and the longer guiding zone. If we launch the laser pulse and the RF pulse just one after another, the last one will continually locate in the amplifying zone of the laser pulse. The guiding regime can be realized if the focusing term in equation suppresses the diffraction divergence term, i.e. the relation

$$(n_\omega-1)k^2R^2>1 \qquad (17)$$

(R is the plasma channel radius) is satisfied. For $\omega=5\times10^{11}$ s^{-1} and $n_e=3\times10^{12}$ cm^{-3} the guiding regime can be realized for channel radius $R\geq1\div2$ cm.

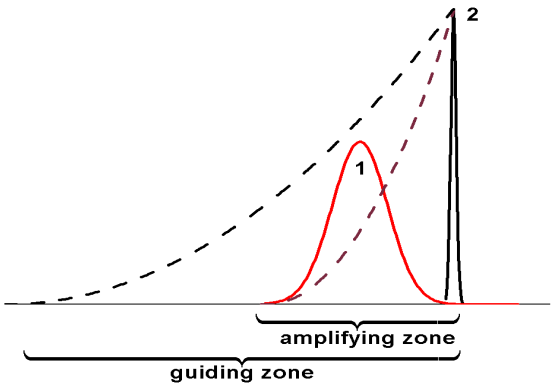

Figure 12. Spatial structure of radio (1) and laser (2) pulses for a given instant of time. Dash curves are the spatial profiles of the gain factor and the refractive index.

Numerical solution of equation (16) was realized the initial temporal profile of the RF pulse

$$E_0(\rho,z=0,\tau=t)=A\times R(\rho)\times\sin^2\left(\pi t/\tau_p\right) \qquad (23)$$

where A is the amplitude of the RF pulse at the axis $\rho=0$, τ_p is its duration, and the function $R(\rho)$ gives the initial radial electric field distribution. Further we assume that $\tau_p=50T$ ($T=2\pi/\omega$), which corresponds to the RF pulse duration of $\tau_p\approx0.628$ ns for $\omega=5\times10^{11}$ s^{-1}. The initial radial distribution $R(\rho)$ was also chosen in the Gaussian form

$$R(\rho)=\exp\left(-\rho^2/2\rho_f^2\right), \qquad (24)$$

where ρ_f is the RF beam radius. The radial profile of the electron density created by KrF laser pulse and determining the value of the gain factor (or absorption coefficient) and the plasma refractive index was also assumed to be Gaussian:

$$n_e(\rho) = n_e(\rho = 0) \times \exp\left(-\rho^2 / 2\rho_e^2\right), \quad (25)$$

At figures 13 and 14 we demonstrate the numerical results of the temporal profile of the intensity of RF pulse for different propagation distances for two values of the initial peak intensity.

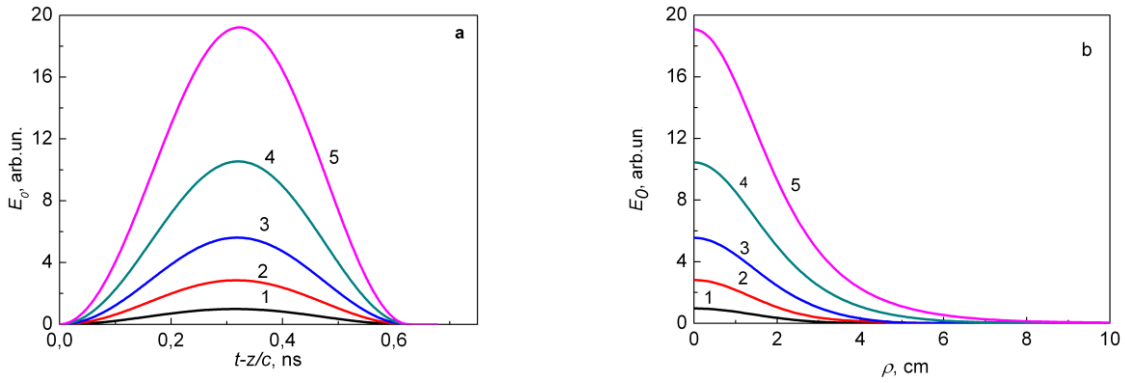

Figure 13. Temporal (1) and radial (2) profiles of the electric field envelope of the amplifying pulse at the different propagation distances z: 1 – 0 cm, 2 – 30 cm, 3 – 60 cm, 4 – 90 cm, 5 – 120 cm. Initial peak intensity is 0.1 W/cm^2.

It can be seen that more significant amplification takes place for the weak initial intensity. For rather intense RF pulses the transported radiation contributed to the EEDF evolution and results in reduction of the gain factor. We see that the trailing edge of the pulse eventually is not amplified.

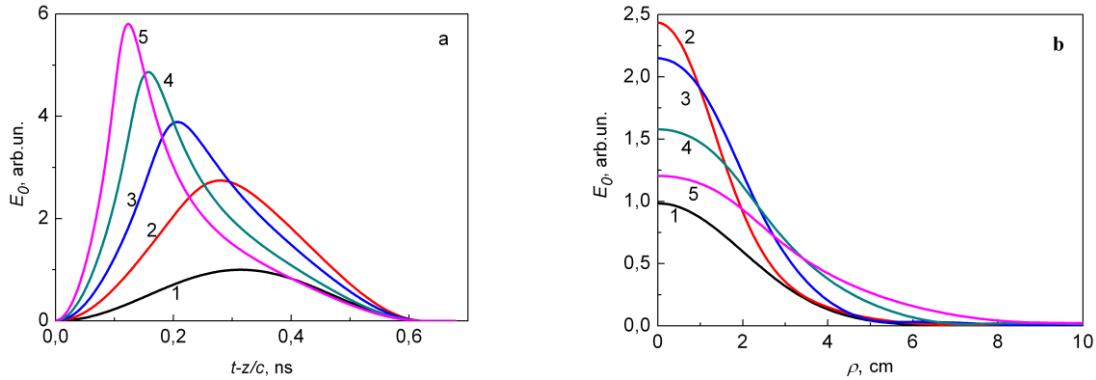

Figure 14. The same, as at figure13, but for the initial peak intensity 1 kW/cm^2.

Conclusions

Thus, it was shown that a plasma channel created in the noble gases by the high intense KrF laser pulse is characterized by the strongly nonequlibrium EEDF which leads to the possibility to use such a channel for amplification of RF radiation. It was demonstrated that xenon plasma has some advantages as the amplifying medium in comparison with other rare gases. Temporal evolution of the gain factor in xenon was investigated. A plasma channel with strongly nonequlibrium EEDF is also characterized by the refractive index greater than unity. The wave equation for the propagation of RF pulses in xenon was solved numerically and analytically. It was shown that such a channel can be considered as a plasma waveguide which can be used for both transportation and amplification of the RF radiation.

Acknowledgments
This work was supported by the Russian Foundation for Basic Research (project no. 15-02-00373). Anna Bogatskaya also thanks the Dynasty Foundation (program for support of students) and the LPI Educational Complex and Special Program of RAS Presidium for young scientist support. Numerical modelling was performed on the SKIF-MSU Chebyshev supercomputer.

References
[1] Agostini P and Di Mauro L F 2004 *Rep. Prog. Phys.* **67** 813
[2] Krausz F and Ivanov M 2009 *Rev. Mod. Phys.* **81** 163
[3] Zhao X M, Wang Y C, Diels J-C and Elizondo J 1995 *IEEE J. Quantum Electron.* **31** 599
[4] Ginzburg V L, Gurevich A V 1960 *Sov. Phys. Usp.* **3** 115
[5] Tzortzakis S, Franco M A, Andre Y-B et al 1999 *Phys. Rev. E* **60**R3505
[6] Rodriguez M, Sauerbrey R, Wille H et al 2002 *Opt. Lett.* **27** 772
[7] Ionin A A, Kudryashov S V, Levchenko A O et al **2012** *Appl. Phys. Lett.* **100** 104105
[8] Penano J, Sprangle P, Hafiz B et al 2012 *J. Appl. Phys.* **111** 033105
[9] Chateauneuf M, Payeur S, Dubois J and Kieffer J-C 2008 *Appl. Phys. Lett.* **92** 091104
[10] Zvorykin V D, Levchenko A O, Smetanin I V and Ustinovski N N 2010 *JETP Lett.* **91** 226
[11] Bogatskaya A V and Popov A M 2013 *JETP Lett.* **97** 388
[12] Bekefi G, Hirshfield Y L and Brown S C 1961 *Phys. Fluids* **4** 173
[13] Bunkin F V, Kazakov A E and Fedorov M V 1973 *Sov. Phys. Usp.* **15** 416
[14] Bogatskaya A V, Volkova E A and Popov A M 2013 *Quantum Electronics* **43** 1110
[15] Fedorov M V, Poluektov N P, Popov A M et al 2012 *IEEE J. Selected Topics in Quantum Electronics* **18** 42